Quality-by-Design-Based Development of Hyaluronic Acid-Conjugated Gemcitabine-Loaded PLGA Nanoparticles for Targeted Anticancer Drug Delivery

Araf Mahefuzabibi Hidayat[1], Dr. Ronak Dedania[2]
[1]*Research Scholar, Department of Pharmaceutical Science, Bhagwan Mahavir Centre for Advance Research, Bhagwan Mahavir University, Surat, Gujarat, India*
[2]*Director, Bhagwan Mahavir Institute of Pharmacy, Bhagwan Mahavir University, Surat, Gujarat, India*

***Abstract*—Purpose: The present study aimed to develop and optimize hyaluronic acid (HA)-conjugated gemcitabine-loaded poly (lactic-co-glycolic acid) (PLGA) nanoparticles for targeted anticancer drug delivery and improved therapeutic performance.**

Methods: PLGA nanoparticle encapsulating gemcitabine was prepared by utilizing the double emulsion-solvent evaporation method. This process was further optimized by employing QbD concept based on response surface methodology. PLGA concentration, PVA concentration, and external aqueous phase volume were chosen as critical process parameters. These optimized PLGA nanoparticles were modified using hyaluronic acid via EDC/NHS conjugation. Various characterizations of the obtained nanoparticles such as particle size, PDI, entrapment efficiency, zeta potential, morphology, drug content, yield, drug release rate, and kinetic study of release were performed.

Results: The optimized OBGEM-2 formulation possessed particle sizes of 225.38 ± 1.69 nm, polydispersity index (PDI) of 0.301 ± 0.016, entrapment efficiency (EE%) of 76.2 ± 0.51%, drug loading capacity of 8.03 ± 0.05%, and production yield of 93.23 ± 1.13%. Scanning electron microscopy studies showed spherical nanoparticles with smooth surfaces. Surface charge measurements by zeta potential showed successful HA conjugation with values of −25.1 ± 3.9 mV. In vitro release studies indicated pH-controlled release characteristics, as 90.78% of the drug was released at pH 5.5 and 64.80% at pH 7.4 after 8 hours of incubation. A diffusion-controlled release mechanism was observed from the in vitro release kinetic profile.

Conclusion: The developed HA-conjugated gemcitabine-loaded PLGA nanoparticles demonstrated favorable physicochemical characteristics, sustained pH-responsive drug release, and good stability, suggesting their potential as a promising targeted delivery system for cancer therapy.

***Index Terms*—Gemcitabine; PLGA nanoparticles; Hyaluronic acid; Targeted drug delivery; Quality by Design; Controlled release; Anticancer therapy**

I. INTRODUCTION

Cancer continues to be one of the most common diseases causing morbidity and mortality, contributing greatly to the burden of diseases around the globe despite major improvements in both diagnosing and treating the disease. Chemotherapy has become an important approach in managing both solid and hematological cancers. Nevertheless, the effectiveness of some anticancer drugs has been constrained by lack of selectivity, quick excretion from the body, toxicity, and resistance. It is for this reason that more advanced drug delivery technologies must be developed to enhance efficacy and reduce toxicity.

Gemcitabine hydrochloride is a pyrimidine nucleoside analog that is frequently used in the therapy of pancreatic, lung, breast, ovarian, and bladder cancer. Gemcitabine achieves its cytotoxic effects by blocking DNA synthesis and initiating cell death in rapidly dividing cancer cells. However, gemcitabine demonstrates several significant pharmacokinetic disadvantages, such as a short duration of action in the bloodstream, degradation via cytidine deaminase enzyme, poor retention in the target tissue, and nonspecific biodistribution in other organs. These factors may cause increased toxicity and low efficiency of the drug.

In recent times, nanoparticle drug delivery systems have gained popularity to counteract such limitations. Of all the biodegradable polymers available, the polymer poly (lactic-co-glycolic acid) (PLGA) is

considered highly attractive due to its superior biocompatibility, biodegradability, control over drug release, and approval for use in pharmaceuticals. PLGA nanoparticles are capable of offering protection to the encapsulated drugs from degradation, prolonging their circulation, and releasing them in a sustained manner.

For increasing tumor specificity even more, there is increasing research into using surface functionalization of nanoparticles for targeting purposes. One interesting molecule for use as a targeting ligand is hyaluronic acid (HA), which is a naturally occurring polysaccharide. The choice is made due to HA's favorable biocompatibility and biodegradability, in addition to a strong binding to CD44 receptors. These CD44 receptors are known to be over-expressed on cancer cells, being involved in tumor progression and metastatic processes, along with drug resistance development.

For the development of nanoparticulate drug delivery systems that meet certain critical quality attributes, there is a need for tight control of formulation variables. Quality by design (QbD) is a scientific approach that has been developed as an innovative tool for developing pharmaceutical products. Through QbD, one is able to identify critical formulation factors and optimize them effectively.

Therefore, the present study aimed to develop and optimize hyaluronic acid-conjugated gemcitabine-loaded PLGA nanoparticles using a Quality-by-Design approach. The prepared nanoparticles were optimized with respect to particle size, polydispersity index, and entrapment efficiency, followed by surface modification with hyaluronic acid. The optimized formulation was further characterized for its physicochemical properties, drug release behavior, release kinetics, and stability to evaluate its potential as a targeted nanoparticulate delivery system for cancer therapy.

II. MATERIALS AND METHODS

2.1 Materials

Gemcitabine Hydrochloride was acquired from Pure chem. Pvt. Ltd. PLGA and Methanol were procured from National chemical, Vadodara. Hyaluronic acid and Potassium dihydrogen phosphate were procured from Astron Chemicals, India. Other laboratory grade materials were bought from an institutional supplier for the manufacturer of reagents and solutions.

2.2 Methods

A. Development of Hyaluronic Acid Conjugated Gemcitabine-PLGA Nanoparticle by Double Emulsion Solvent Evaporation Method

The double emulsion solvent evaporation method ($W_1/O/W_2$) is particularly suitable for the formulation of gemcitabine-loaded PLGA nanoparticles due to the hydrophilic nature of gemcitabine. In this method, gemcitabine is first dissolved in an internal aqueous phase (W_1) to ensure uniform drug distribution. This aqueous drug solution is then emulsified into an organic phase containing PLGA dissolved in a volatile organic solvent, forming a primary water-in-oil (W_1/O) emulsion using probe sonication or high-speed homogenization. The primary emulsion is subsequently added to an external aqueous phase (W_2) containing polyvinyl alcohol as a stabilizer to produce a water-in-oil-in-water ($W_1/O/W_2$) double emulsion. Continuous stirring facilitates evaporation of the organic solvent, leading to polymer solidification and entrapment of gemcitabine within the PLGA matrix. The resulting nanoparticles are collected by centrifugation, washed to remove unentrapped drug and residual stabilizer, and finally dried or redispersed. This technique enables effective encapsulation of gemcitabine, controlled particle size, and sustained drug release, making it highly suitable for developing PLGA-based nanoparticulate systems for anticancer drug delivery.

B. Coating of nanoparticle with hyaluronic acid

Bonding the hyaluronic acid carboxylic group to the chitosan amino group was performed using EDC as the coupling factor. Briefly, the optimized NPs in terms of EE% and size (according to the Design-Expert software) were suspended in PBS (pH 7.4). Accordingly, EDC was added to the HA solution and then the mixture was added dropwise to PLGA NPs on a magnetic stirrer at 400 rpm in the environment temperature for 1 h. The obtained solution was centrifuged (18,000rpm) at 10°C for 30min to separate NPs. The deposit of nanoparticles was washed with Distilled Water to remove any probable unreacted materials around and on NPs.

C. Optimization of Hyaluronic Acid Conjugated Gemcitabine-PLGA Nanoparticle by Quality by design approach

Optimization of the gemcitabine-loaded PLGA nanoparticle formulation was carried out using a Quality by Design-based statistical approach to identify the most suitable combination of formulation variables that yields nanoparticles with desired characteristics. Based on preliminary trials and process understanding, three critical formulation factors were selected as independent variables: PLGA concentration (X_1), PVA concentration (X_2), and external aqueous phase volume (W_2) (X_3), each studied at predetermined low and high levels. The effect of these variables on key responses, namely particle size (Y_1), polydispersity index (Y_2), and entrapment efficiency (Y_3), was systematically evaluated using response surface methodology. Experimental runs were generated by the design software and prepared using the double emulsion solvent evaporation method while keeping the drug amount, internal aqueous phase (W_1), and organic solvent volume constant across all batches. The experimental results were fitted to polynomial regression models, and analysis of variance was applied to determine the significance of model terms and assess model adequacy. Numerical optimization was then performed using the desirability function approach, wherein particle size and PDI were minimized and entrapment efficiency was maximized to obtain an optimum formulation. The optimized formulation was finally prepared in replicate and evaluated to confirm the predicted responses and establish a robust design space for reproducible nanoparticle production.

D. Characterization of Conjugation Using Zeta Potential

Zeta potential devices are designed to assess the surface charge of nanoparticles, whether they are in a liquid or a solid form. In this study, the surface charges of the conjugated nanoparticles were examined using the Zetasizer Nano ZS by Malvern Instruments Ltd. The analysis involved taking zeta measurements at 25 °C, utilizing 1. 5 mL of the conjugated nanoparticles. Each test was conducted with a folded capillary zeta cell, which required a 1-minute equilibration period at 25 °C before measurements began.

E. Characterization of Optimized Gemcitabine Loaded Hyaluronic Acid Conjugated PLGA Nanoparticles

Particle Size and PDI

Particle size and polydispersity index (PDI) of the prepared gemcitabine-loaded PLGA nanoparticles were determined using dynamic light scattering (DLS) technique. The measurements were carried out using a zeta sizer after appropriate dilution of the nanoparticle dispersion with distilled water to avoid multiple scattering effects. The particle size was expressed as the Z-average diameter, which represents the intensity-weighted mean hydrodynamic diameter of the nanoparticles. The polydispersity index was used as an indicator of the width of the particle size distribution and formulation homogeneity. All measurements were performed in triplicate at a controlled temperature, and the results were reported as mean ± standard deviation. A low PDI value indicated a narrow and uniform particle size distribution, confirming good colloidal stability and reproducibility of the nanoparticle formulation.

Entrapment Efficiency (%EE)

The encapsulation efficiency of gemcitabine within PLGA nanoparticles was determined to evaluate the extent of drug entrapment in the polymeric matrix. A known volume of the freshly prepared nanoparticle dispersion was centrifuged at high speed to separate the nanoparticles from the unencapsulated free drug present in the supernatant. The clear supernatant was carefully collected and analyzed for gemcitabine content using a suitable UV–visible spectrophotometric method at the predetermined λmax. Encapsulation efficiency was calculated by subtracting the amount of free drug detected in the supernatant from the total amount of drug initially added during formulation, using the following equation:

$$\%EE = \frac{Total\ drug\ added - Free\ drug}{Total\ drug\ added} \times 100$$

All measurements were performed in triplicate, and the results were expressed as mean ± standard deviation. This method provides a reliable estimation of drug loading within the PLGA nanoparticles and reflects the effectiveness of the formulation process.

Morphological Analysis by Transmission Electron Microscopy (TEM)

Nanoparticle morphology was examined using Transmission Electron Microscopy (TEM). The

nanoparticle suspension was diluted with distilled water and sonicated to obtain a uniform dispersion. A drop of the diluted sample was placed on a carbon-coated copper grid and allowed to stand for 2 min. Excess liquid was removed using filter paper, and the grid was air-dried at room temperature. The prepared sample was analyzed using TEM operated at an accelerating voltage of 200 kV. Particle size and morphology were determined from the obtained micrographs.

% Drug Content

The percentage drug content of the optimized gemcitabine-loaded PLGA nanoparticle formulation was determined to assess the uniformity of drug distribution within the nanoparticles. An accurately weighed quantity of the dried nanoparticle sample was dissolved in a suitable solvent system capable of completely solubilizing both the polymer and the drug. The resulting solution was filtered or centrifuged to remove any insoluble residues and analyzed for gemcitabine content using a validated UV–visible spectrophotometric method at the selected wavelength. The percentage drug content was calculated by comparing the experimentally determined drug concentration with the theoretical drug content using the following expression:

$$\%\ Drug\ content = \frac{Amount\ of\ drug\ present}{Theoretical\ amount\ of\ drug} \times 100$$

All determinations were carried out in triplicate, and the results were expressed as mean ± standard deviation. This evaluation ensured consistency, accuracy, and reproducibility of drug loading in the nanoparticle formulation.

% Yield

The percentage yield of the gemcitabine-loaded PLGA nanoparticles was determined to evaluate the efficiency of the formulation process. After completion of nanoparticle preparation and drying, the final weight of the obtained nanoparticles was accurately measured. The percentage yield was calculated by comparing the actual weight of nanoparticles recovered with the total theoretical weight of all solid components used in the formulation, including the drug and polymer, using the following equation:

$$\%\ Yield = \frac{Weight\ of\ obtained\ nanoparticles}{Weight\ of\ drug + Weight\ of\ polymer} \times 100$$

The experiment was performed in triplicate, and the results were expressed as mean ± standard deviation. A high percentage yield indicates minimal material loss during processing and confirms the suitability and reproducibility of the nanoparticle preparation method.

In-vitro Drug Release Studies for Optimized Nanoparticles

The in-vitro drug release behavior of the optimized gemcitabine-loaded PLGA nanoparticles was evaluated to assess the release pattern and pH-responsive performance of the formulation. The study was carried out using a dialysis membrane method under controlled conditions. An accurately measured amount of nanoparticle dispersion equivalent to a known quantity of gemcitabine was placed in a dialysis bag, which was securely sealed and immersed in release medium maintained at 37 ± 0.5 °C with continuous stirring. Release studies were performed in buffer solutions of pH 5.5 and pH 7.4 to simulate the tumor microenvironment and physiological conditions, respectively.

At predetermined time intervals, aliquots of the release medium were withdrawn and replaced with an equal volume of fresh buffer to maintain sink conditions. The collected samples were analyzed for gemcitabine content using a validated UV–visible spectrophotometric method. The cumulative percentage of drug released was calculated and plotted as a function of time. All experiments were conducted in triplicate, and the results were expressed as mean ± standard deviation. This study provided insight into the sustained and pH-dependent release characteristics of the optimized nanoparticle formulation, supporting its potential application in targeted anticancer drug delivery.

Evaluation of Release Rate Kinetics

To understand the drug release mechanism from the optimized gemcitabine-loaded PLGA nanoparticles, the in-vitro release data were fitted to standard kinetic models. The cumulative percentage drug release versus time data were analyzed using zero-order (cumulative % release vs time), first-order (log % drug remaining vs time), Higuchi model (cumulative % release vs square root of time), and Korsmeyer–Peppas model (log cumulative % release vs log time). The best-fit model was identified based on the highest correlation coefficient (R^2) and minimum residual error.

Stability Study

Stability studies of the optimized gemcitabine-loaded PLGA nanoparticle formulation were conducted to evaluate its physical and chemical stability during storage. The formulation was stored under accelerated stability conditions (40 ± 2 °C / 75 ± 5% RH) for a defined period. At predetermined intervals, samples were withdrawn and evaluated for appearance, particle size, polydispersity index, zeta potential, entrapment efficiency, and drug content to monitor any changes in physicochemical properties.

The stability of the optimized formulation was further assessed by comparing the in-vitro drug release profile before and after storage under accelerated conditions. Any variation in release behavior was analyzed to determine the effect of storage on drug release performance. All studies were carried out in triplicate, and the results were expressed as mean ± standard deviation. This stability evaluation ensured that the optimized gemcitabine-loaded PLGA nanoparticles retained acceptable quality attributes and performance over time, supporting their suitability for further development and potential therapeutic application.

III. RESULT AND DISCUSSION

3.1 Formulation of Gemcitabine-loaded hyaluronic acid conjugated PLGA nanoparticles

Gemcitabine-loaded PLGA nanoparticles were prepared by a double emulsion solvent evaporation method. First, 10 mg of gemcitabine hydrochloride was accurately weighed and dissolved in 1 mL of distilled water to form the inner aqueous phase (W_1). Separately, PLGA was dissolved in 5 mL of dichloromethane to obtain the organic phase (O). The amount of PLGA in this phase was varied according to the experimental design, typically in the range of 25-75 mg, corresponding to concentrations of 5-15 mg/mL. The gemcitabine solution (W_1) was then added slowly into the PLGA solution under gentle stirring and the mixture was emulsified using a probe sonicator in an ice bath for about 30 seconds at around 40% amplitude to form a fine primary W_1/O emulsion. For the external aqueous phase (W_2), polyvinyl alcohol (PVA) was dissolved in distilled water at different concentrations (0.5–1.5% w/v) as per the design. The volume of the PVA solution was varied between 25 and 50 mL while keeping the organic phase fixed at 5 mL, which corresponds to organic-to-external phase ratios in the range of approximately 1:5 to 1:10. This PVA solution was kept under magnetic stirring at about 800–1000 rpm. The freshly prepared W_1/O emulsion was then poured slowly into the PVA solution under high-speed stirring and immediately subjected to a second probe sonication step in an ice bath for around 60 seconds at 40% amplitude to produce a stable $W_1/O/W_2$ double emulsion. The resulting emulsion was stirred magnetically at about 600 rpm for approximately 3 hours at room temperature to allow complete evaporation of the organic solvent, leading to the formation of gemcitabine-loaded PLGA nanoparticles dispersed in the PVA solution.

The nanoparticle dispersion was purified by centrifugation. The emulsion was transferred into centrifuge tubes and centrifuged at 15,000 rpm for 20 minutes. The supernatant containing free drug and excess PVA was discarded and the nanoparticle pellet was redispersed in distilled water. This washing step was repeated two more times to remove residual PVA and unentrapped gemcitabine. Finally, the purified nanoparticles were resuspended in distilled water or suitable buffer and the volume was adjusted to 10 mL. This dispersion of gemcitabine-loaded PLGA nanoparticles was used for characterization and for further surface modification with hyaluronic acid.

Table 1 Optimization Parameters and Evaluation Data of Gemcitabine-loaded PLGA nanoparticles

Std.	Sr. No	Independent Variables			Dependent Variables		
		PLGA conc.	PVA conc.	O: W_2 ratio	PS (nm)	PDI	% EE
15	1	10	1	37.5	170.2	0.271	66.41
8	2	15	1	50	190.4	0.31	74.51
11	3	10	0.5	50	147.7	0.223	58.21
3	4	5	1.5	37.5	1657	0.312	64.53
1	5	5	0.5	37.5	175.1	0.279	65.85
9	6	10	0.5	25	213.4	0.264	76.49
2	7	15	0.5	37.5	195.6	0.289	77.56
10	8	10	1.5	25	227.4	0.365	85.64

6	9	15	1	25	280.4	0.423	89.45
4	10	15	1.5	37.5	195.7	0.287	76.54
7	11	5	1	50	170.4	0.24	62.07
16	12	10	1	37.5	170.9	0.265	67.41
12	13	10	1.5	50	193.9	0.312	77.45
14	14	10	1	37.5	170.9	0.245	65.14
5	15	5	1	25	180.7	0.277	67.77
13	16	10	1	37.5	170.4	0.254	66.53

All 13 Gemcitabine-loaded PLGA nanoparticles formulations were prepared according to the experimental design, and the primary responses like, particle size (nm), PDI and %EE were measured. As shown in Table 1, the actual particle sizes ranged from 170 nm to 280 nm, and the % EE ranges from 58 % to 89% which validated the robustness of the statistical model.

The Fraction of Design Space (FDS) plot illustrates the relationship between the prediction uncertainty, expressed as standard error of the mean, and the fraction of the design space considered. The curve shows a gradual increase in standard error as the fraction of design space increases, indicating that prediction uncertainty is lowest near the center of the design space and increases toward its boundaries. The horizontal reference line represents the acceptable limit of standard error, while the vertical line indicates the fraction of design space that satisfies this criterion. In the present study, the FDS value of 0.94 suggests that approximately 94% of the design space lies within the acceptable prediction uncertainty limit. The calculated standard error mean (0.796) remains below the defined threshold, confirming that the developed models provide reliable and precise predictions across a large portion of the design space. Overall, this plot demonstrates the robustness of the established design space and supports its suitability for consistent and reproducible formulation of gemcitabine-loaded PLGA nanoparticles.

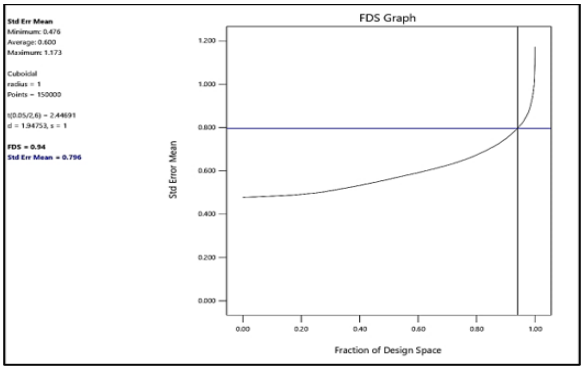

Figure 1 Fraction of Design Space (FDS) plot

A. Model fitting and regression analysis

Model fitting and regression analysis were performed to establish a reliable mathematical relationship between the formulation variables and the critical quality attributes of gemcitabine-loaded PLGA nanoparticles. The experimental data were fitted to a second-order polynomial regression model, and the suitability of the model was evaluated using analysis of variance. The significance of the model was confirmed by high F-values and statistically significant p-values, indicating that the selected independent variables adequately explained the observed variations in particle size, polydispersity index, and entrapment efficiency. Good agreement between predicted and experimental values, along with satisfactory coefficients of determination and low residual errors, demonstrated the robustness and predictive capability of the regression models, supporting their use for formulation optimization and design space development.

Different mathematical models, including linear, two-factor interaction (2FI), quadratic, and cubic models, were evaluated for each response to identify the most appropriate model describing the formulation behavior. Model selection was based on a combination of statistical indicators, namely low standard deviation, minimum PRESS value, and the highest values of R^2, adjusted R^2, and predicted R^2. As shown in table 2, For particle size (Y_1), the quadratic model showed excellent performance with a very low standard deviation, near-perfect R^2 values, and the lowest PRESS value compared to linear and 2FI models, indicating superior fitting and predictive accuracy. Similarly, for polydispersity index (Y_2), the quadratic model demonstrated a substantial improvement over lower-order models, with markedly higher R^2 values and minimal PRESS, confirming its suitability to explain variations in size distribution.

In the case of entrapment efficiency (Y_3), although linear and 2FI models showed moderate fitting, the quadratic model provided better explanatory power

with improved R^2 and acceptable PRESS values, justifying its selection for further analysis. Cubic models, despite showing high R^2 values in some cases, were identified as aliased by the software and were therefore excluded from the final selection to avoid overfitting and lack of model interpretability. Overall, the quadratic model was consistently selected for all responses, as it offered the best balance between model adequacy, predictive reliability, and statistical robustness, making it suitable for optimization and design space development.

Table 2 Model Selection Summery

Responses	Models	SD	R^2	Adjusted R^2	Predicted R^2	PRESS	Selection
Y_1: PS	Linear	37.12	0.878	0.847	0.794	27796.01	
	2FI	42.85	0.878	0.796	0.583	56324.69	
	Quadratic	1.81	1.000	1.000	0.999	113.573	Suggested
	Cubic	2.18	1.000	0.999		*	Aliased
Y2: PDI	Linear	0.160	0.391	0.239	0.131	0.438	
	2FI	0.184	0.392	-0.013	-0.424	0.717	
	Quadratic	0.018	0.996	0.991	0.980	0.010	Suggested
	Cubic	0.022	0.9972	0.986		*	Aliased
Y3: EE	Linear	6.000	0.770	0.713	0.629	697.480	Aliased
	2FI	6.840	0.776	0.626	0.307	1301.520	
	Quadratic	4.890	0.924	0.809	0.311	1294.950	Suggested
	Cubic	4.850	0.963	0.812		*	
Model was selected based on Low PRESS value, Low SD, Highest R^2							
Software have also suggested Aliased models too, which was omitted from selection criteria							

The below table 3 presents the regression coefficients and corresponding p-values obtained from the full and reduced quadratic models for particle size (Y_1), polydispersity index (Y_2), and entrapment efficiency (Y_3). The full models include linear, interaction, and quadratic terms, while the reduced models retain only statistically significant terms based on p-values and overall model adequacy. For particle size (Y_1), all linear and quadratic terms (X_1, X_2, X_3, X_{11}, X_{22}, and X_{33}) were highly significant ($p < 0.05$), whereas interaction terms showed non-significant effects and were omitted in the reduced model. In the case of PDI (Y_2), strong significance was observed for linear and quadratic terms, confirming the influence of formulation variables on size distribution, while interaction terms were excluded due to lack of statistical significance. For entrapment efficiency (Y_3), linear effects of PLGA concentration, PVA concentration, and W_2 volume were significant, along with selected quadratic terms, whereas interaction effects were statistically insignificant and therefore removed. Overall, the reduced models preserve the dominant effects governing each response while improving model simplicity and interpretability without compromising predictive performance.

Table 3 Regression Analysis Using ANOVA

Model term	Y1: PS			Y2: PDI			Y3: % EE		
	Full model		Reduced Model	Full model		Reduced Model	Full model		Reduced Model
	coefficient	p-value	Coefficient	Coefficient	p-value	Coefficient	Coefficient	p-value	Coefficient
C	242.425	< 0.0001	242.425	0.18425	< 0.0001	< 0.0001	61.74	0.0098	61.49
X1	100.4625	< 0.0001	100.4625	0.0525	0.0002	< 0.0001	7.99	0.0036	7.99
X2	-58.5125	< 0.0001	-58.5125	0.0325	0.002	0.0004	9.02	0.002	9.02
X3	36.15	< 0.0001	36.15	0.14425	< 0.0001	< 0.0001	-5.96	0.0137	-5.96
X1X2	-0.45	0.6375		0.00475	0.6102		-0.5625	0.8257	
X1X3	-0.125	0.8949		-0.00425	0.6476		1.41	0.5859	

X2X3	-1.375	0.1803		-0.01025	0.2901		0.5025	0.844	
X11	49.7375	< 0.0001	49.7375	0.20725	< 0.0001	< 0.0001	-0.4975	0.8455	
X22	40.3875	< 0.0001	40.3875	0.14175	< 0.0001	< 0.0001	-5.42	0.0687	-5.42
X33	-4.5375	0.0024	-4.5375	0.11425	< 0.0001	< 0.0001	-6.31	0.0418	-6.31

The regression analysis presented in the table provides clear insight into the individual and combined effects of formulation variables on particle size (Y_1), polydispersity index (Y_2), and entrapment efficiency (Y_3). For particle size, the positive coefficient of PLGA concentration (X_1) and W_2 volume (X_3) indicates that increasing these factors leads to an increase in particle size, whereas the negative coefficient of PVA concentration (X_2) suggests a size-reducing effect due to improved stabilization of the emulsion system. The significant positive quadratic terms (X_{11} and X_{22}) reflect a nonlinear increase in particle size at higher levels of PLGA and PVA, while the negative quadratic term for W_2 volume (X_{33}) indicates a size-limiting effect at higher external phase volumes. The interaction terms were not statistically significant, indicating that particle size is predominantly governed by individual factor effects rather than their interactions.

For polydispersity index, all three linear terms exhibited positive coefficients, demonstrating that increases in PLGA concentration, PVA concentration, and W_2 volume contribute to broader size distribution. The significant quadratic terms further indicate nonlinear behavior, suggesting that extreme levels of these variables adversely affect size uniformity. The absence of significant interaction effects implies that PDI is mainly controlled by the magnitude of individual formulation parameters rather than synergistic effects between them.

In the case of entrapment efficiency, PLGA concentration and PVA concentration showed positive effects, indicating improved drug encapsulation with increasing polymer and stabilizer levels. In contrast, the negative coefficient of W_2 volume suggests reduced entrapment efficiency at higher external aqueous phase volumes, likely due to enhanced drug diffusion into the continuous phase. The significant negative quadratic terms for PVA concentration and W_2 volume indicate a decline in entrapment efficiency beyond optimal levels, reflecting saturation and drug loss phenomena. Overall, the table demonstrates that linear and quadratic effects dominate the formulation behavior, justifying the selection of reduced quadratic models for optimization and design space establishment.

The contour and three-dimensional surface plots illustrate the combined influence of PLGA concentration (A) and PVA concentration (B) on the critical quality attributes, while the W_2 volume was maintained constant at its center level (figure 2). For particle size, both contour and surface plots show a clear increase in particle size with increasing PLGA concentration, whereas higher PVA concentration tends to reduce particle size due to improved emulsification and stabilization. The smooth curvature of the surface confirms a significant quadratic effect and minimal interaction between the two variables.

In the case of polydispersity index, the plots demonstrate that PDI increases gradually with increasing PLGA and PVA concentrations, indicating broader size distribution at higher levels of formulation variables. Lower PLGA and PVA concentrations result in narrower size distribution, as reflected by lower PDI values. The nearly planar response surface suggests dominant linear effects with moderate quadratic contribution.

For entrapment efficiency, the contour and surface plots reveal an increase in %EE with rising PLGA and PVA concentrations, highlighting enhanced drug encapsulation at higher polymer and stabilizer levels. However, the curvature observed in the response surface indicates that beyond an optimal range, further increases may not proportionally improve entrapment. Overall, these plots confirm that PLGA and PVA concentrations play a critical role in governing nanoparticle characteristics and support the selected optimization region identified through desirability analysis.

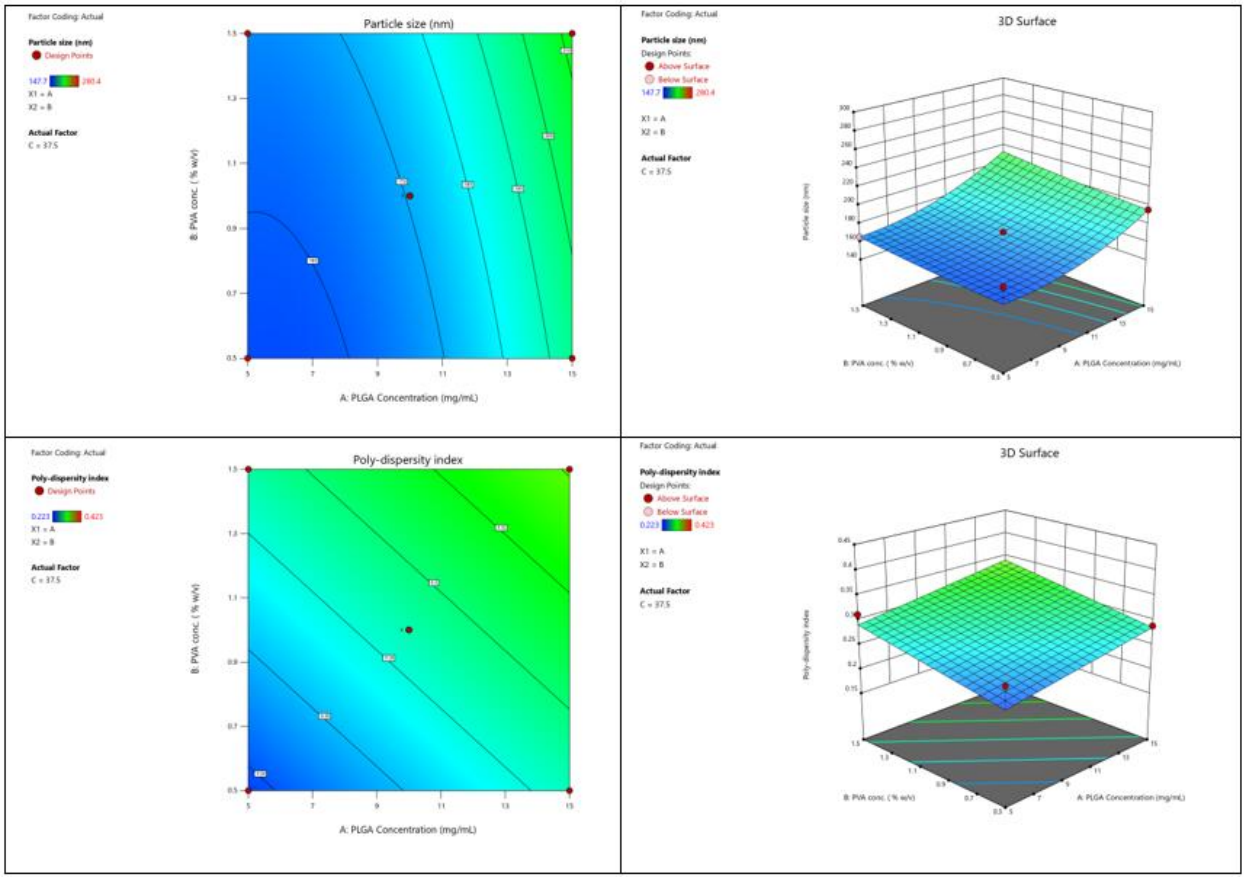

Figure 2 3D Surface Plots and Contour Plots for Responses Y1, Y2 and Y3

The interaction plot (figure 3) for particle size shows that particle size increases with increasing PLGA concentration at both low and high PVA levels. The nearly parallel nature of the lines indicates a weak interaction between PLGA and PVA concentration, confirming that particle size is primarily governed by the main effects of individual factors rather than their combined interaction. Higher PVA concentration slightly moderates the increase in particle size by improving emulsion stabilization. For polydispersity index, the interaction plot reveals a gradual increase in PDI with increasing PLGA concentration at both PVA levels. The close-to-parallel trend of the lines suggests minimal interaction between PLGA and PVA, indicating that size distribution is mainly influenced by the independent contribution of each variable. Lower PVA concentration consistently results in lower PDI values, reflecting better size uniformity. In the case of entrapment efficiency, %EE increases with increasing PLGA concentration at both low and high PVA levels, with a steeper slope observed at higher PVA concentration. This indicates a modest interaction effect, where increased stabilizer concentration enhances drug entrapment at higher polymer levels. Overall, these plots support the statistical findings that interaction effects are limited, while linear and quadratic effects dominate the formulation behavior.

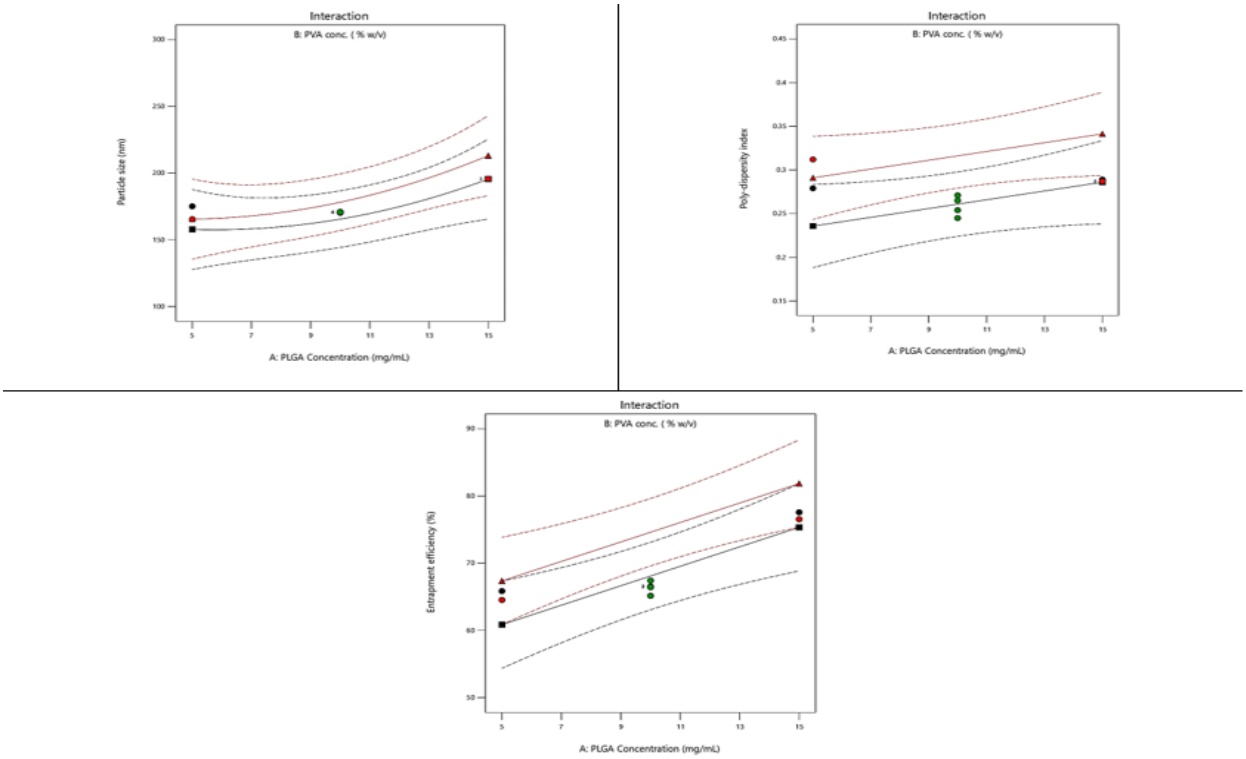

Figure 3 Interaction Plot

The overlay plot identifies the design space where all predefined criteria for particle size, polydispersity index, and entrapment efficiency are simultaneously satisfied. The highlighted yellow region represents the optimal formulation window, indicating that moderate PLGA concentration combined with lower PVA concentration yields nanoparticles with acceptable size, narrow size distribution, and high entrapment efficiency. This region confirms the robustness of the optimized formulation and defines a reliable operating range for reproducible nanoparticle production.

B. Checkpoint analysis and formulation optimization

The overlay plot identifies the design space where all predefined criteria for particle size, polydispersity index, and entrapment efficiency are simultaneously satisfied. The highlighted yellow region represents the optimal formulation window, indicating that moderate PLGA concentration combined with lower PVA concentration yields nanoparticles with acceptable size, narrow size distribution, and high entrapment efficiency. This region confirms the robustness of the optimized formulation and defines a reliable operating range for reproducible nanoparticle production.

The table 4 resents the numerical optimization and experimental validation of the optimized gemcitabine-loaded PLGA nanoparticle formulations. Two optimized batches (OBGEM-1 and OBGEM-2) were prepared using formulation variables predicted by the desirability function, both achieving an overall desirability value of 1, indicating complete fulfillment of the predefined optimization criteria. The selected factor levels for PLGA concentration (X_1), PVA concentration (X_2), and W_2 volume (X_3) lie within the established design space, confirming the robustness of the optimization strategy. For both batches, the predicted values of particle size, polydispersity index, and entrapment efficiency were in close agreement with the experimentally observed values. The experimentally obtained particle sizes were slightly higher than the predicted values; however, the percentage error remained below 3% for all responses, demonstrating excellent predictive accuracy of the developed regression models. Similarly, the PDI and entrapment efficiency values showed minimal deviation between predicted and experimental results, with percentage errors well within acceptable limits. The low prediction errors and consistent experimental performance across replicate measurements (n = 3)

confirm the reliability and validity of the optimization process. These results verify that the developed models are capable of accurately predicting formulation behavior and that the optimized gemcitabine-loaded PLGA nanoparticles can be reproducibly prepared within the defined design space.

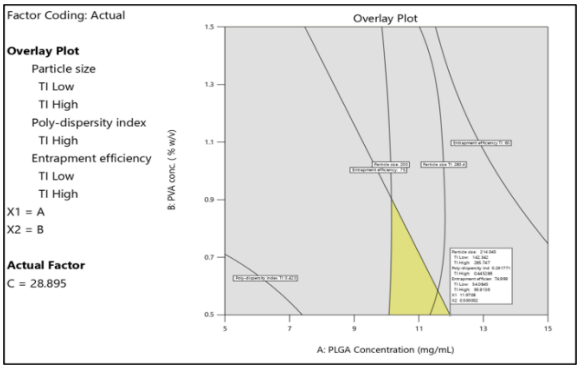

Figure 4 Overlay Plot

Table 4 Checkpoint Analysis and Optimization Results

Batch code	Factor value	Desirability	Predicted value			Experimental value*			% Error		
			PS (nm)	PDI	EE (%)	PS (nm)	PDI	EE %	PS (nm)	PDI	EE %
OBGEM 1	X1=11.97, X2= 0.500, X3= 28.89	1	214.05	0.292	75	219.8	0.302	77.21	2.68	3.42	2.94
OBGEM 2	X1=12.11, X2= 0.500, X3= 29.09	1	220.12	0.28	75.11	225.4	0.289	75.48	2.39	3.21	0.49
*All values are mean ± SD (n = 3)											

The DoE data were utilized to identify which of the three batches of checkpoints had desirability 1 for checkpoint assessment. OBGEM 2, with the lowest error percentage compared to batches 1, was therefore selected as the final optimized batch.

C. Characterization of Optimized Gemcitabine Loaded Hyaluronic Acid Conjugated PLGA Nanoparticles

1. Particle Size and Polydispersity Index (PDI)

The optimized formulation OBGEM-2 exhibited a Z-average particle size of 225.4 nm with a polydispersity index of 0.289, indicating a narrow and uniform particle size distribution. Dynamic light scattering analysis showed a single dominant intensity peak, confirming the absence of aggregation and a monomodal distribution pattern. The result quality was rated as good, supported by a high intercept value (0.853), reflecting reliable correlation data. Triplicate measurements demonstrated excellent reproducibility, with a mean particle size of 225.38 ± 1.69 nm and a mean PDI of 0.301 ± 0.016. These results confirm the consistency and stability of the optimized nanoparticle formulation, making it suitable for further characterization and application.

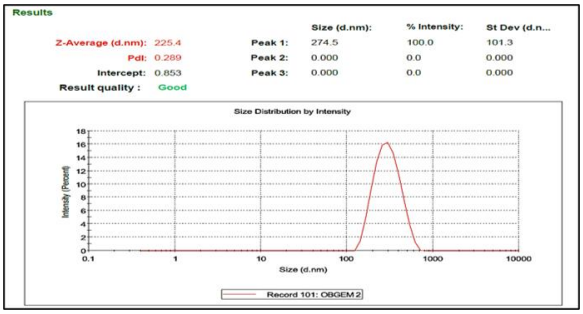

Figure 5 Particle Size Analysis and PDI of Optimized Batch of NP

2. Entrapment Efficiency (%EE)

The optimized batch OBGEM-2 showed high and consistent drug entrapment, with individual entrapment efficiency values of 75.48%, 76.54%, and 76.58% (table 5). The mean entrapment efficiency was 76.2% with a low standard deviation of 0.51, indicating good reproducibility and minimal batch-to-batch variation in drug loading.

Table 5 Result of Entrapment Efficiency for Gemcitabine Nanoparticle Optimized Batch

Batch	% Entrapmenrt Efficiency			Mean	SD
OBGEM 2	75.48	76.54	76.58	76.2	0.509379

3. % Yield

The optimized batch OBGEM-2 showed a high production yield, with individual yield values of 91.65%, 94.25%, and 93.78%. The mean yield was 93.23% with a standard deviation of 1.13, indicating good process efficiency and reproducibility of the nanoparticle formulation method.

Table 6 Result of Yield Determination for Gemcitabine Nanoparticle Optimized Batch

Batch	Yield (%)			Mean	SD
OBGEM 2	91.65	94.25	93.78	93.23	1.13

4. % Drug Content

The optimized batch OBGEM-2 demonstrated uniform drug content, with individual values of 8.10%, 7.97%, and 8.03%. The mean drug content was 8.033% with a very low standard deviation of 0.053, indicating excellent content uniformity and consistency of drug distribution within the nanoparticles.

Table 7 Result of Drug Content Determination of Optimized Batch

Batch	% Drug Content			Mean	SD
OBGEM 2	8.1	7.97	8.03	8.033	0.053

5. Morphological Analysis by TEM

TEM analysis demonstrated that the formulated nanoparticles possessed a predominantly spherical morphology with sizes in the nanometer range. The particles were well-formed and exhibited distinct boundaries, confirming successful nanoparticle formation. Minor aggregation was observed, which may be attributed to particle-particle interactions during sample drying. The micrograph further indicated a relatively uniform morphology, supporting the suitability of the formulation for targeted drug delivery applications.

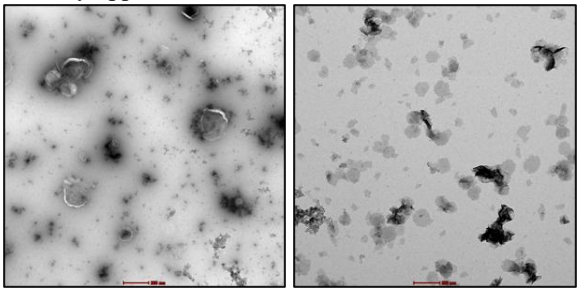

Figure 6 SEM Image of Optimized Batch (OBGEM-2)

D. Surface modification of optimized nanoparticles with hyaluronic acid (HA)

The optimized gemcitabine-loaded PLGA nanoparticle dispersion was used for hyaluronic acid coating. An amount of nanoparticle dispersion equivalent to approximately 50 mg of PLGA (calculated from the formulation used for the optimized batch) was taken and the volume was adjusted to 10 mL with 0.1 M MES buffer (pH 5.5). This suspension was kept under gentle magnetic stirring. To activate the surface carboxyl groups of PLGA, EDC and NHS were added to the nanoparticle suspension at final concentrations of about 4 mg/mL and 2.4 mg/mL, respectively, and the mixture was stirred for 30 minutes at room temperature to allow formation of the NHS-activated ester on the particle surface.

Separately, 10 mg of hyaluronic acid was dissolved in 5 mL of MES buffer (pH 6.5–7.0) to obtain a clear HA solution. After the activation period, the HA solution was added slowly to the activated nanoparticle suspension under gentle stirring, giving an approximate HA: PLGA weight ratio of 1:5. The reaction mixture was then stirred at room temperature for 4 hours to allow covalent attachment of HA to the PLGA nanoparticles through amide bond formation. During this period the dispersion was protected from light and excessive foaming.

After completion of the coupling reaction, the HA-coated nanoparticles were purified by centrifugation at 15,000 rpm for 20 minutes. The supernatant containing unbound HA and residual EDC/NHS was discarded and the pellet was redispersed in distilled water. This washing step was repeated two times to ensure complete removal of free HA and reaction by-products. Finally, the purified HA-coated gemcitabine-loaded PLGA nanoparticles (Gem-PLGA–HA NPs) were resuspended in distilled water or suitable buffer to the desired volume and stored at 4 °C until further characterization.

1. Characterization of HA-CS conjugation by Zeta Potential

The zeta potential of the optimized HA-coated gemcitabine-loaded PLGA nanoparticles was found to be −25.1 ± 3.9 mV, with the distribution showing a single narrow peak at approximately −21.1 mV and the instrument indicating good result quality. The dispersion had a conductivity of 0.741 mS/cm. The

shift to a distinctly negative surface charge after coating is consistent with the presence of hyaluronic acid, whose carboxyl groups are ionized at the measurement pH, and confirms successful surface modification. A zeta potential of around −25 mV suggests that the nanoparticles possess sufficient electrostatic repulsion to remain physically stable against aggregation during storage. The presence of a single sharp peak in the zeta potential distribution further indicates a homogeneous nanoparticle population without evidence of multiple surface-charge subpopulations.

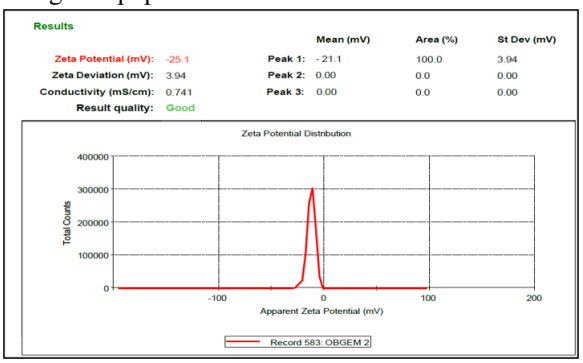

Figure 7 Zeta Potential of Optimized Nanoparticle Batch (OBGEM-2)

2. In-Vitro Drug Release Studies

The in-vitro drug release study demonstrated a sustained and pH-dependent release pattern for all formulations over an 8-hour period. HA-GEM-PLGA nanoparticles exhibited a faster and higher cumulative drug release at pH 5.5 compared to pH 7.4, indicating enhanced drug release under acidic conditions that mimic the tumor microenvironment. At pH 5.5, HA-GEM-PLGA showed a cumulative release of 90.78% at 8 h, whereas only 64.80% drug release was observed at pH 7.4, confirming the pH-responsive behavior of the formulation. Similarly, GEM-CS nanoparticles showed greater drug release at pH 5.5 (74.96% at 8 h) compared to pH 7.4 (53.67%), although the overall release was comparatively lower than that of HA-GEM-PLGA formulations. The enhanced release from HA-coated PLGA nanoparticles can be attributed to increased polymer swelling and partial destabilization of the carrier under acidic conditions, along with the hydrophilic nature of hyaluronic acid. Overall, the release profiles confirm that HA-GEM-PLGA nanoparticles provide controlled and preferential drug release in acidic environments, supporting their potential for tumor-targeted drug delivery.

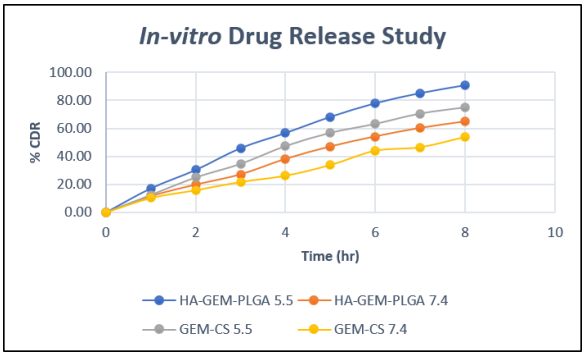

Figure 8 %CDR of Optimized Batch

3. Evaluation of Release Kinetics

The data was analysed for various kinetic models viz. zero order, Higuchi, first order, Korsmeyer-Peppas etc. The release kinetics graph showed maximum linearity in the case of Korsmeyer-Peppas and Higuchi release. In Korsmeyer-Peppas release model the 'n' value was found to be less than 1 i.e., it signifies a non fickian release implying the release to be through erosion and diffusion of the matrix which is seen in optimized (OBGEM 2) batch.

Table 8 Release Kinetics of Optimized Batch Nanoparticles

Batch	Zero order	First order	Higuchi	K-P		H-C
	R^2	R^2	R^2	R^2	n	R^2
In-vitro						
HA-CS-EXT-NPs in pH 5.5						
HA-PLGA-GEM-NPs	0.962	0.978	0.942594	0.9943	9.000	0.994

4. Stability Study

The short-term stability study of the optimized HA-GEM-PLGA nanoparticle formulation was carried out under accelerated conditions, and the results indicate acceptable physicochemical stability over the study period. Initially, the formulation appeared clear with no visible lumps, confirming good dispersion. After one month, the formulation remained clear, while a slight haze was observed at 1.5 months, suggesting minor physical changes without visible aggregation or precipitation. A marginal increase in particle size was observed after one month (from 225.38 ± 5 nm to

232.23 ± 5 nm), which may be attributed to slight polymer relaxation or surface hydration during storage. Interestingly, a reduction in particle size at 1.5 months (192 ± 5 nm) suggests possible restructuring or redistribution of loosely associated particles. The PDI values showed only a slight increase over time (0.301 to 0.323), remaining within an acceptable range and indicating preservation of a relatively uniform size distribution. Zeta potential values showed a small decrease in magnitude over time, but remained sufficiently negative, suggesting continued electrostatic stability of the nanoparticles. Entrapment efficiency showed a moderate decline after storage, decreasing from 76.21% initially to approximately 68% after one and 1.5 months. This reduction may be due to slow drug diffusion from the polymeric matrix during storage. However, drug content remained nearly constant throughout the study, indicating minimal drug degradation and good chemical stability of gemcitabine within the formulation.

The in-vitro drug release profiles in acidic medium (pH 5.5) before and after one month of storage showed comparable release behaviour. The cumulative drug release of the stored formulation was slightly higher at later time points compared to the freshly prepared optimized batch. This minor increase in release rate may be associated with subtle changes in polymer matrix structure or surface characteristics during storage. Importantly, the overall sustained and pH-responsive release pattern was preserved, confirming that storage under accelerated conditions did not adversely affect the release performance. The stability data demonstrate that the optimized HA-GEM-PLGA nanoparticles maintain acceptable physical integrity, drug content, and release characteristics over the tested period, supporting their suitability for further development and extended stability evaluation.

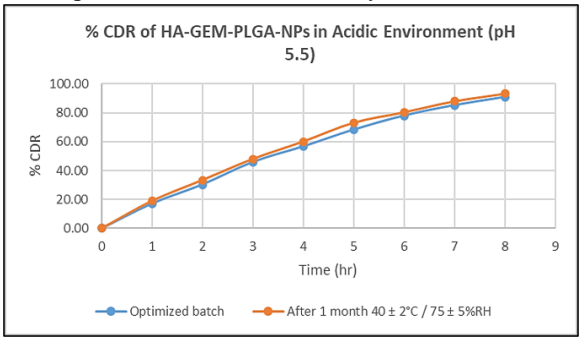

Figure 9 % CDR for Accelerated Study Sample

IV. CONCLUSION

The present study successfully developed and optimized gemcitabine-loaded hyaluronic acid-conjugated PLGA nanoparticles (HA-GEM-PLGA NPs) for targeted cancer drug delivery. The optimized formulation (OBGEM-2) exhibited desirable physicochemical characteristics, including a particle size of 225.38 ± 1.69 nm, PDI of 0.301 ± 0.016, entrapment efficiency of 76.2%, drug content of 8.033%, and high production yield of 93.23%, indicating uniformity, reproducibility, and efficient drug encapsulation. SEM analysis confirmed the formation of discrete, spherical nanoparticles with smooth morphology, while zeta potential analysis (−25.1 ± 3.9 mV) verified successful hyaluronic acid surface conjugation and good colloidal stability. The in-vitro drug release studies demonstrated a sustained and pH-responsive release pattern, with significantly higher drug release at acidic pH 5.5 (90.78%) compared to physiological pH 7.4 (64.80%), supporting selective release in the tumor microenvironment. Release kinetic modeling indicated a non-Fickian diffusion mechanism involving both diffusion and matrix erosion. Stability studies further confirmed that the formulation maintained acceptable physical integrity, drug content, and release characteristics under accelerated storage conditions, despite a slight reduction in entrapment efficiency over time. Overall, these findings suggest that the optimized HA-GEM-PLGA nanoparticle system is a stable, efficient, and promising targeted delivery platform for gemcitabine, with significant potential to enhance therapeutic efficacy and tumor-specific drug delivery in cancer treatment.

Conflict of interest: The authors disclose that they have no conflicting financial interests.

ACKNOWLEDGEMENT

Authors would like to thank Dr. Vineet C. Jain and Bhagwan Mahavir college of Pharmacy for offering research facility that is required in this study. We also thanks to Dr. Zarana Dedania and Dr. Ronak Dedania for providing all technical guidance.

REFERENCES

[1] Pujari R, Sah SK, Bhatt S. Introduction to lung cancer. In: Immunotherapy Against Lung Cancer: Emerging Opportunities and Challenges. Springer; 2024. p. 1–9.

[2] Kosmidis PA. Introduction to lung cancer. In: Imaging in Clinical Oncology. Springer; 2013. p. 169–.

[3] Manegold C. Gemcitabine (Gemzar®) in non-small cell lung cancer. Expert Rev Anticancer Ther. 2004;4(3):345–360.

[4] Du X, Luo W, Li H, Gu Q, Huang P, Wang C, et al. Hsa_circ_0125356 promotes gemcitabine resistance by modulating WNT canonical and non-canonical pathways via miR-582-5p/FGF9 axis in non-small cell lung cancer. 2025;24(1):59.

[5] Patel P, Shoyele NO, Shoyele SA. Preparation and evaluation of meclinertant-loaded PLGA/chitosan nanoparticles as a potential treatment for non-small cell lung cancer using A549 cells. J Drug Deliv Sci Technol. 2025;107:106831.

[6] Kesharwani P, Kumar V, Goh KW, Gupta G, Alsayari A, Wahab S, et al. PEGylated PLGA nanoparticles: unlocking advanced strategies for cancer therapy. 2025;24(1):205.

[7] Chen KW, Huang HL, Wang CC, Hsiao CH, Lee YC, Lu ZB, et al. Innovative design of hyaluronic acid conjugated polymeric drug for targeted therapy of non-small cell lung cancer. 2025;318:144874.

[8] Mohabbat A, Dadashi H, Mashinchian M, Karimian-Shaddel A, Adibkia K, Nazemiyeh H, et al. Hyaluronic acid-functionalized PEG-PLGA nanoparticles for targeted shikonin delivery: A potential therapeutic approach for prostate cancer. 2025;15(4):1–15.

[9] Patel N, Patel PJ. QbD-driven formulation development and evaluation of genistein nanoparticles for prostate cancer. Recent Adv Drug Deliv Formul. 2025;19(1):53–71.

[10] Zhang Q, Liu T, Qiao F, Li W, Hou C. Hyaluronic acid–chitosan conjugated PLGA nanoparticles for dual chemo-photothermal therapy of triple-negative breast cancer. Sci Rep. 2025.

[11] Hlaing SP, Cao J, Lee J, Kim J, Saparbayeva A, Kwak D, et al. Hyaluronic acid-conjugated PLGA nanoparticles alleviate ulcerative colitis via CD44-mediated dual targeting to inflamed colitis tissue and macrophages. 2022;14(10):2118.

[12] La Verde G, Sasso A, Rusciano G, Capaccio A, Fusco S, Mayol L, et al. Characterization of hyaluronic acid-coated PLGA nanoparticles by surface-enhanced Raman spectroscopy. 2022;24(1):601.

[13] Parkkola H. Hyaluronic acid-coated gold nanoparticles as an anticancer drug delivery system: Biological characterization and efficacy. 2015.

[14] Nizzolo S. Derivatization and characterization of polysaccharides to be used for the functionalization of biomaterials. 2026.

[15] Worsley GJ, Kumarswami N, Minelli C, Noble JE. Characterisation of antibody conjugated particles and their influence on diagnostic assay response. Anal Methods. 2015;7(22):9596–9603.

[16] James AE, Driskell JD. Monitoring gold nanoparticle conjugation and analysis of biomolecular binding with nanoparticle tracking analysis (NTA) and dynamic light scattering (DLS). Analyst. 2013;138(4):1212–1218.

[17] Song X, Zhao Y, Hou S, Xu F, Zhao R, He J, et al. Dual agents loaded PLGA nanoparticles: Systematic study of particle size and drug entrapment efficiency. Eur J Pharm Biopharm. 2008;69(2):445–453.

[18] Wu C, Szymanski C, McNeill J. Preparation and encapsulation of highly fluorescent conjugated polymer nanoparticles. Langmuir. 2006;22(7):2956–2960.

[19] Pecher J, Mecking S. Nanoparticles of conjugated polymers. Chem Rev. 2010;110(10):6260–6279.

[20] Di Pasqua AJ, Mishler RE II, Shi YL, Dabrowiak JC, Asefa T. Preparation of antibody-conjugated gold nanoparticles. Mater Lett. 2009;63(21):1876–1879.

[21] Dudhwala YD, Kapoor DU, Mehta RK, Shah DP, Ramani VD, Dedania RR, et al. Strategic formulation and optimization of a febuxostat nanoparticles infused topical gel using quality-by-design principles for enhanced therapeutic

efficacy in gout management. 2025;10(34):e00972.
[22] Patel BB, Ramani VD, Dudhawala YD, Mehta RK. Folic acid-conjugated chitosan nanoparticles for colon-targeted delivery of imatinib mesylate. 2026;16(6):369.
[23] Chowdhury S, Yusof F, Faruck MO, Sulaiman N. Process optimization of silver nanoparticle synthesis using response surface methodology. Powder Technol. 2016;148:992–999.
[24] Weng J, Tong HH, Chow SF. In vitro release study of the polymeric drug nanoparticles: Development and validation of a novel method. Pharmaceutics. 2020;12(8):732.
[25] Lomis N, Westfall S, Farahdel L, Malhotra M, Shum-Tim D, Prakash S. Human serum albumin nanoparticles for use in cancer drug delivery: Process optimization and in vitro characterization. Nanomaterials. 2016;6(6):116.
[26] Zhang J, Li S, An FF, Liu J, Jin S, Zhang JC, et al. Self-carried curcumin nanoparticles for in vitro and in vivo cancer therapy with real-time monitoring of drug release. 2015;7(32):13503–13510.
[27] Modi S, Anderson BD. Determination of drug release kinetics from nanoparticles: Overcoming pitfalls of the dynamic dialysis method. Mol Pharm. 2013;10(8):3076–3089.
[28] Lemoine D, François C, Kedzierewicz F, Préat V, Hoffman M, Maincent P. Stability study of nanoparticles of poly(ε-caprolactone), poly(D,L-lactide) and poly(D,L-lactide-co-glycolide). Biomaterials. 1996;17(22):2191–2197.
[29] Wang Y, Zhu L, Dong Z, Xie S, Chen X, Lu M, et al. Preparation and stability study of norfloxacin-loaded solid lipid nanoparticle suspensions. 2012;98:105–111.
[30] Selvamani V. Stability studies on nanomaterials used in drugs. In: Characterization and Biology of Nanomaterials for Drug Delivery. Elsevier; 2019. p. 425–444.